ACS APPLIED MATERIALS & INTERFACES

Research Article

www.acsami.org

Parallel Carbon Nanotube Stripes in Polymer Thin Film with Remarkable Conductive Anisotropy

Jinrui Huang,[†,‡] Yutian Zhu,[*,†] Wei Jiang,[*,†] Jinghua Yin,[†] Qingxin Tang,[§] and Xiaodong Yang[∥]

[†]State Key Laboratory of Polymer Physics and Chemistry, Changchun Institute of Applied Chemistry, Chinese Academy of Sciences, Changchun 130022, People's Republic of China

[‡]University of Chinese Academy of Sciences, Beijing 100049, People's Republic of China

[§]Key Laboratory of UV Light Emitting Materials and Technology under Ministry of Education, Northeast Normal University, Changchun 130024, People's Republic of China

[∥]Changchun Institute of Technology, Changchun 130012, People's Republic of China

Supporting Information

ABSTRACT: In our previous study (Mao et al. *J. Phys. Chem. Lett.* **2013**, *4*, 43−47), we proposed a novel method, that is, the shear-flow-induced hierarchical self-assembly of two-dimensional fillers (octadecylamine-functionalized graphene) into the well-ordered parallel stripes in a polymer matrix, to fabricate the anisotropic conductive materials. In this study, we extend this method to one-dimensional multiwalled carbon nanotubes (MWCNTs). Under the induction of shear flow, the dispersed poly(styrene ethylene/butadiene-styrene) (SEBS) phase and MWCNTs can spontaneously assemble into well-ordered parallel stripes in the polypropylene (PP) thin film. The electrical measurements indicate that the electrical resistivity in the direction parallel to the stripes is almost 6 orders of magnitude lower than that in the perpendicular direction, which is by far the most striking conductive anisotropy for the plastic anisotropic conductive materials. In addition, it is found that the size of the MWCNT stripe as well as the electrical property of the resulting anisotropic conductive thin film can be well-controlled by the gap of the shear cell.

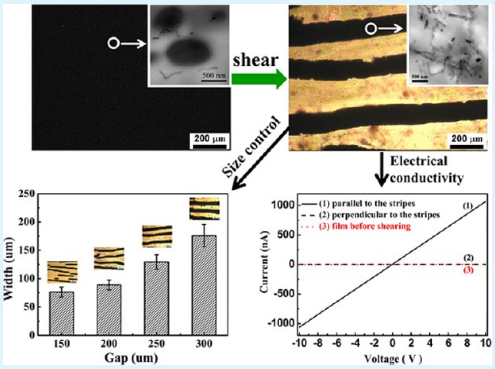

KEYWORDS: *conductive anisotropy, carbon nanotube, shear flow, hierarchical assembly, thin film*

1. INTRODUCTION

Carbon nanotubes (CNTs), long cylinders of covalently bonded carbon atoms, have received much attention owing to their unique qualities, such as low mass density, high flexibility, and remarkable mechanical, electrical, and thermal properties.[1] Because of its extraordinary electrical property, the CNT is widely used to blend with polymer to fabricate conductive polymer composites.[1,2] Normally, the resulting conductive polymer composite is isotropic in electrical property because conductive fillers are randomly distributed in the polymer matrix. Recently, however, much attention has been paid to fabricate the anisotropic conductive polymer materials because of their immense potential applications in various fields.[3] Generally, two strategies were developed to fabricate the anisotropic conductive polymer materials. One strategy is to make the conductive filler orientate in the polymer matrix, which endows the material with the anisotropic properties.[4−10] For example, de Heer et al.[4] utilized a ceramic filter to make CNTs perpendicular to the thin film surface firstly. Then, the CNTs were parallel to the surface after gently rubbing the film along the surface with an aluminum foil. The resistivity measurements of these films showed obvious conductive anisotropy in the directions along and normal to the aligned tubes. Moreover, Cheng and co-workers[6] reported that the graphite nanosheets oriented intensively in the composite under the shear, which led to the anisotropic properties of the composite. Another strategy for the fabrication of anisotropic conductive composites is to make the conductive fillers assemble into ordered one-dimensional (1D) chain- or stripe-like assemblies in the polymer matrix. On the basis of this strategy, several methods, including self-assembly of block copolymer with nanoparticles,[11] templated synthesis,[12−14] and the external fields such as magnetic-field- and electric-field-induced assembly,[15−23] were developed to produce these 1D structured materials. For instance, Zhu and co-workers fabricated the ordered 1D chain assembles by the assembly of graphene-encapsulated multifunctional magnetic composite microspheres in a uniform magnetic field.[23]

Recently, we proposed a simple, but efficient, method to prepare 1D stripes of graphene (GE) in PP thin film via shear-induced self-assembly.[24] In that work, it was found that GE nanosheets and SEBS spontaneously aggregated into ordered

Received: October 27, 2013
Accepted: January 3, 2014
Published: January 3, 2014

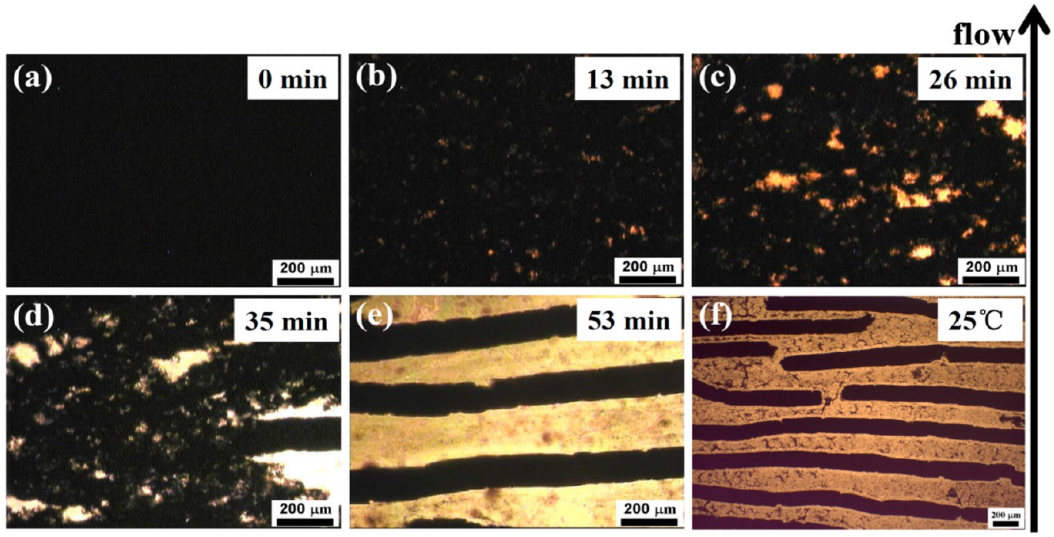

Figure 1. Optical micrographs of the PP/SEBS/1.5 wt % MWCNTs composite at a shear rate of 0.05 s^{-1} with different shearing times and the sample after cessation of the flow and cooling to the room temperature: (a) 0 min; (b) 13 min; (c) 26 min; (d) 35 min; (e) 53 min; (f) the film at 25 °C. The gap is fixed at 250 μm. The temperature for (a)−(e) is fixed at 280 ± 1 °C. The micrographs of (a)−(e) were obtained from the Linkam CSS 450 stage equipped with an Olympus BX-51 optical microscope. The micrograph of (f) was from the ZEISS AXIO Imager A2m optical microscope.

parallel stripes under the shear flow. The electrical measurements revealed that the electrical resistivity in the direction parallel to the GE stripes was almost 4 orders of magnitude lower than that in the direction vertical to the GE stripes. To the best of our knowledge, this is the most significant anisotropy for the anisotropic conductive polymer materials. However, the conductive anisotropy still needs to be further enhanced because the electrical resistivity along the GE stripes is as high as 3.5×10^5 Ω·m. Moreover, it is still not clear whether this method is suitable for other nanofillers with different shapes. Therefore, we chose a totally different conductive nanofiller (1D MWCNT) to prepare the anisotropic conductive polymer materials containing 1D MWCNT stripes.

2. EXPERIMENTAL SECTION

2.1. Material. The polymers used in this study are polypropylene (PP) and poly(styrene ethylene/butadiene-styrene) (SEBS). PP (140) with an M_n of 7.74×10^4 g/mol and the polydispersity index (M_w/M_n) of 5.47 was supplied by Jilin Petrochemical (China). SEBS (Kraton G1652) was obtained from the Shell Development. Its weight-average molecular weight (M_w) is about 45 000 g/mol, and the styrene content is ca. 29 wt %. MWCNTs (diameter: 10−20 nm; length: 5-15 μm; purity: >95%) were purchased from Shenzhen Nanotech Port Co. Ltd.

2.2. Preparation of PP/SEBS/1.5 wt % MWCNTs Composite. The PP/SEBS/1.5 wt % MWCNTs composite was prepared by melt compounding in a co-rotating twin-screw minicompounder (DSM Microcompounder). In this study, the weight ratio of PP/SEBS was fixed at 90/10 and the loading content of MWCNTs was 1.5 wt %. Prior to melt compounding, all materials were dried in a vacuum oven at 80 °C for 24 h. PP and MWCNTs were mixed first by melt blending in the minicompounder at 200 °C and 100 rpm for 9 min. Then, SEBS was rapidly added into the melting PP/MWCNTs mixture and mixed for 1 min. Finally, the resulting PP/SEBS/1.5 wt % MWCNTs melt was injection molded into plates with a thickness of 1 mm and a diameter of 25 mm using a DSM microinjection molding machine with fixing the barrel temperature and mold temperature at 200 and 30 °C, respectively. The injection molding pressure and holding pressure were set at 3 and 5 bar, respectively.

2.3. Fabrication of PP/SEBS/1.5 wt % MWCNTs Anisotropic Conductive Thin Film. The shear-induced self-assembly of randomly distributed MWCNTs into parallel MWCNT stripes was performed by employing a Linkam CSS 450 stage equipped with an Olympus BX-51 optical microscope. The morphological evolution of the PP/SEBS/1.5 wt % MWCNTs mixture under the shear flow was online visualized and recorded. The sample was held in the gap between the two quartz disks. The internal surfaces of both the quartz disks were covered by the polyimide thin films to prevent adhesion of the PP/SEBS/1.5 wt % MWCNTs composites to the quartz disks. The experiments were performed at 280 ± 1 °C, and the applied shear rate was kept constant at 0.05 s^{-1}. To examine the effect of the gap between the two quartz disks on the formation of MWCNT stripe, its value was varied from 150 to 300 μm. After a period of shear, the ordered parallel MWCNT stripes were formed. Then, the shear flow was stopped and the stage temperature was decreased to freeze the well-ordered stripe structure. The resulting anisotropic thin film was peeled from the polyimide film at room temperature.

2.4. Characterization. The internal structures of PP/SEBS/1.5 wt % MWCNTs composite and the MWCNT stripes in the PP/SEBS/1.5 wt % MWCNTs anisotropic conductive thin film were characterized by transmission electron microscopy (TEM). TEM measurements were performed on a JEOL JEM-1011 transmission electron microscope operated at an acceleration voltage of 100 kV. To prepare the TEM sample, the PP/SEBS/1.5 wt % MWCNTs composite was ultra-microtomed in liquid nitrogen with a thickness of ~50 nm by a microtome (LEICA ULTRACUTR ME_1-057) equipped with a glass knife. To characterize the internal structure of the MWCNT stripes in the thin film, the stripe was embedded in epoxy resin first and then was ultra-microtomed in liquid nitrogen with a thickness of ~50 nm by a microtome equipped with a glass knife.

To visualize the morphology of the resulting anisotropic thin film, we examined the sample by the classic optical microscopy (ZEISS AXIO Imager A2m). The mode we used was transmission mode. The width and length of the stripes were obtained by iTEM 5.1 (Build 1276, Olympus Soft Imaging Solutions GmbH) from a large number of optical micrographs.

Electrical resistivity measurements of thin films were performed by the conventional two-point probe technique using a computer-controlled Keithley 4200 semiconductor parameter analyzer. All the measurements were performed at room temperature. Before the measurements, two gold electrodes (2.0 mm × 0.5 mm) were sputtered onto the film with a spacing of 1.5 mm in the direction parallel or perpendicular to the stripes. For comparison, the same

electrical resistivity measurement was also performed for the isotropic thin film without the shear-induced self-assembly.

3. RESULTS AND DISCUSSION

In our previous studies,[24,25] it was found that both the two-dimensional (2D) filler (GE) and the three-dimensional (3D) filler (the microsized polyamide 6 droplet) can spontaneously assemble into well-ordered parallel stripes in the PP thin film via the shear induction. However, it is still not clear whether this method is applicable for other conductive nanofillers with completely different shapes because the shape of the assemble unit may influence the formation of the parallel-stripe structure. In the current study, we selected an entirely different conductive filler (1D MWCNT) to fabricate the multifunctional anisotropic materials. In Figure 1, we present a series of optical images to visualize the formation and evolution of MWCNT stripes under the shear flow. Figure 1a shows the initial state of the PP/SEBS/1.5 wt % MWCNTs composite before shear-induced assembly. Clearly, the optical image is completely black and opaque to light because MWCNTs are randomly distributed in the sample. Under the shear flow at a rate of 0.05 s^{-1}, MWCNTs and SEBS form some randomly distributed loose aggregates at first (Figure 1b–d), and then assemble into the well-ordered parallel MWCNT stripes aligned vertical to the shear direction (Figure 1e). Subsequently, the plastic thin film containing parallel MWCNT stripes is obtained by cooling the sample to room temperature after cessation of the shear flow, as shown in Figure 1f. Figure 2

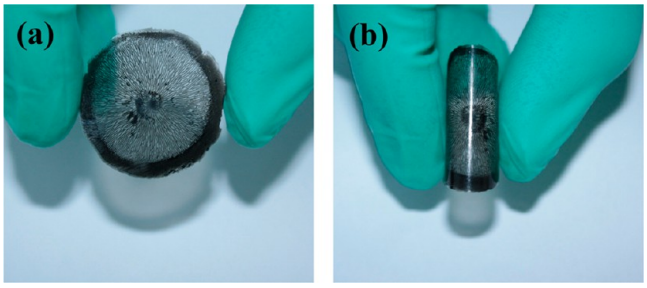

Figure 2. Digital camera images of the resulting plastic anisotropic conductive thin film: (a) an unbent plastic anisotropic conductive thin film; (b) bent plastic anisotropic thin film.

shows the typical digital camera images of the resulting plastic anisotropic conductive thin film containing parallel MWCNT stripes. Interestingly, the thin film could be freely bent and folded. This is critically important for the application of the material in the flexible device. The formation of the MWCNT stripe is attributed to the cooperation of several important factors. First, small SEBS droplets tend to coalesce into bigger droplets at the shear rate of 0.05 s^{-1}. During the coalescence, SEBS acts as a "glue" to adhere MWCNTs together to form the aggregates. Second, it has been reported that the growth of the clusters or stripes perpendicular to the flow direction is attributed to the existence of negative normal stress (N_1).[24−29] When $N_1 < 0$, the dispersed phase is compressed in the flow direction. Moreover, the confinement effect imposed by the upper and lower disks also limits the growth of the stripe in the gradient direction. As a result, the MWCNT stripe can only grow and align along the vorticity direction. To better understand the formation of the parallel MWCNT stripe under the shear flow, we present a video to show this dynamic process in the Supporting Information (Movie S1).

The internal microstructure of the MWCNT stripe is visualized by the TEM technique. The TEM images of the initial PP/SEBS/1.5 wt % MWCNTs composite as well as the self-assembled MWCNT stripe are presented in Figure 3. For

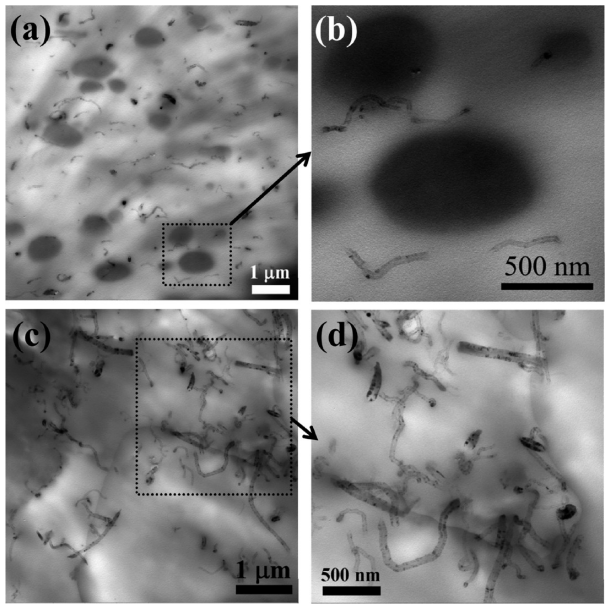

Figure 3. TEM images of the initial PP/SEBS/1.5 wt % MWCNTs composite and the stripe in the anisotropic film that was obtained after the shear-induced assembly: (a) the initial PP/SEBS/1.5 wt % MWCNTs composite, (b) partial enlarged image of (a), (c) the cross-sectional view of the stripe, (d) partial enlarged image of (c). Bright region at (a) and (b): PP phase. Gray domains at (a) and (b): SEBS phase.

the initial PP/SEBS/1.5 wt % MWCNTs composite, it is clear that both the MWCNTs and the SEBS (gray spheres) are uniformly distributed in the PP matrix (bright region), as shown in Figure 3a,b. For the TEM images of the MWCNT stripe (Figure 3c,d), however, MWCNTs are enriched and randomly distributed in the SEBS phase, which is similar to the GE stripes in our previous study.[24]

Because of the high electrical conductivity of MWCNTs and the parallel MWCNT stripe structure in PP thin film, it is expected that this PP thin film will show significant anisotropy in electrical property. In Figure 4, we present the $I-V$ curves for the resulting PP/SEBS/1.5 wt % MWCNTs anisotropic film (curves 1 and 2). For comparison, the $I-V$ curve of the initial

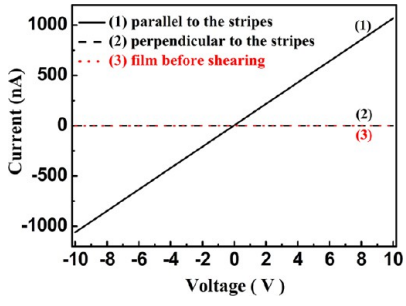

Figure 4. $I-V$ curves of the PP/SEBS/1.5 wt % MWCNTs anisotropic film in the directions (1) parallel and (2) perpendicular to the stripes. (3) $I-V$ curve of the isotropic PP/SEBS/1.5 wt % MWCNTs composite film before shearing.

isotropic PP/SEBS/1.5 wt % MWCNTs film without the shear-induced assembly is also included, as shown in Figure 4 (curve 3). In the direction parallel to the MWCNT stripe (curve 1), the $I-V$ curve shows a linear Ohmic behavior because of the existence of a conductive MWCNT network in the stripe. However, an insulating behavior is observed in the direction perpendicular to the stripes (curve 2) because all the MWCNTs are enriched in the MWCNT stripes. For the initial PP/SEBS/1.5 wt % MWCNTs film before the shear-induced assembly (curve 3), the $I-V$ curve also exhibits an insulating behavior. This is because the loading of MWCNT in the current study is lower than its electrical percolation threshold in the PP matrix. According to the $I-V$ curves in Figure 4, the determined electrical resistivity along the MWCNT stripes is ca. 2.41×10^3 Ω·m. In the direction perpendicular to the MWCNT stripes, however, the determined electrical resistivity is ca. 1.78×10^9 Ω·m, which is about 6 orders of magnitude higher than that in the direction parallel to the stripes. Clearly, the anisotropy in the electrical resistivity of the resulting PP/SEBS/1.5 wt % MWCNTs multifunctional plastic film is more remarkable than that of the reported PP/SEBS/GE film (ca. 4 orders of magnitude difference in the electrical resistivity).[24] In our previous study, the used GE has a relatively low electrical conductivity (2.6 S/m), which was synthesized from the reduction of octadecylamine-functionalized graphite oxide. However, the MWCNT used in the current study has a relatively high electrical conductivity of 705.6 S/m. Therefore, the resulting MWCNT stripes have a relatively low electrical resistivity than that of the GE stripes.

From the optical micrograph of the MWCNT stripes (Figure 1f), it is clear that the stripes have a distribution in length and width. Figure 5a,b presents the distributions of the width and length of MWCNT stripes that are derived from a large number of optical micrographs of the resulting MWCNT stripes at a gap of 250 μm. The results of statistics show that the MWCNT stripes have an average length of 3.57 mm and an average width of 129 μm. Precise control of the stripe structure, such as its width and length, is critical to the future application of the materials. At a gap of 250 μm, the resulting anisotropic thin film has a thickness of 160 μm. Clearly, the width of the stripe is comparable to the thickness of the thin film. Therefore, the width of the stripe can be easily adjusted by changing the gap between the upper and lower disks. Figure 6 shows the dependence of the width and length of the MWCNT stripe on the gap. The formation and evolution of the MWCNT stripe at the gap of 150, 200, and 300 μm are elucidated by a series of optical micrographs, as shown in the Supporting Information (Figures S1–S3). As expected, the width of the stripe increases as the gap is increased (Figure 6a). More interestingly, it is also found that the length of stripe is increased with the gap. Clearly, the wider the stripe, the less fracture the stripe will be. As a result, the wide stripe is usually longer than the thin stripe, as shown in Figure 6b.

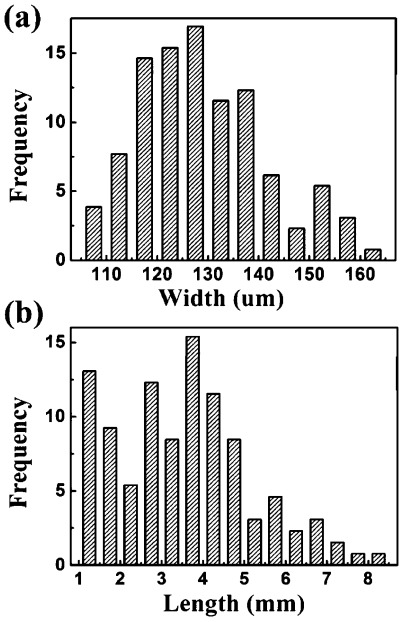

Figure 5. Histograms of the width and length distributions of the stripes obtained by analyzing optical micrographs of the PP/SEBS/1.5 wt % MWCNTs anisotropic films fabricated by shear-flow-induced assembly at the gap of 250 μm: (a) histogram of the width distribution; (b) histogram of the length distribution. The total number of stripes used in the statistical analysis is about 130.

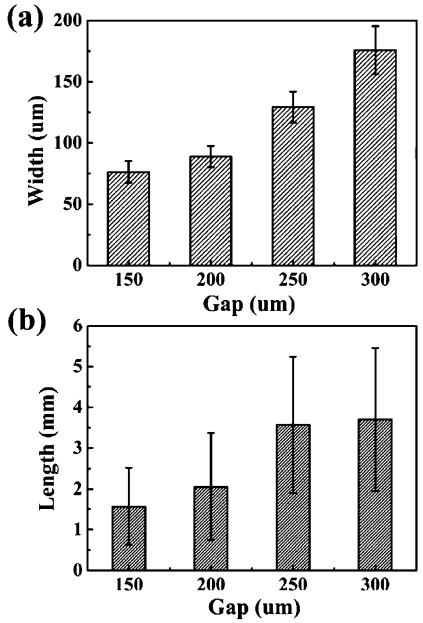

Figure 6. Effect of gap on the size of the stripes: (a) the width of the stripes; (b) the length of the stripes in the anisotropic films.

Because the width and length of the MWCNT stripe depend on the gap, the electrical resistivity of the stripe would be changed with the gap. Figure 7 shows the variation of the

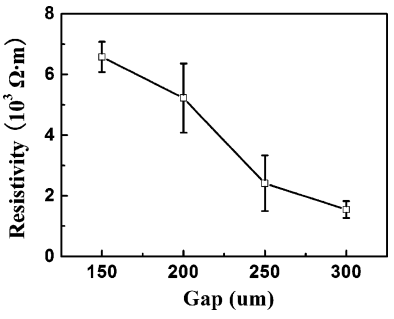

Figure 7. Effect of the gap on the electrical resistivity along the MWCNT stripes in the anisotropic films.

dx.doi.org/10.1021/am404758d | ACS Appl. Mater. Interfaces 2014, 6, 1754–1758

electrical resistivity in the direction parallel to the MWCNT stripes with the gap. The electrical resistivities for the samples at different gaps are presented in the Supporting Information (Table S1). As the gap is increased, the electrical resistivity of the MWCNT stripe is decreased. This may be because the MWCNT network in the stripe will be more perfect as the width of the stripes is increased.

4. CONCLUSIONS

In the current study, we fabricate an anisotropic conductive polymer film by shear-flow inducing MWCNTs to assemble into well-ordered parallel MWCNT stripes vertical to the shear flow. The electrical measurement shows that the electrical resistivity along the MWCNT stripes is 6 orders of magnitude lower than that orthogonal to the stripes, which exhibits an outstanding conductive anisotropy. In addition, the parallel structure of the MWCNT stripes can be well-controlled by changing the gap of the shear cell. It is observed that the width and length of the stripes increase as the gap is increased. This result indicates that shear-flow-induced hierarchical self-assembly could be a universal method for the fabrication of the multifunctional anisotropic materials since we have successfully extended this method from the 2D (GE) and 3D (PA6 droplet) fillers to the 1D filler (MWCNT).

■ ASSOCIATED CONTENT

Supporting Information

A movie showing the dynamic process of the formation of MWCNT stripe, a series of optical images for the formation and evolution of MWCNT stripes at a gap of 150, 200, and 300 μm under the shear flow, and the electrical resistivities for the samples at different gaps. This material is available free of charge via the Internet at http://pubs.acs.org.

■ AUTHOR INFORMATION

Corresponding Authors

*E-mail: ytzhu@ciac.ac.cn. Phone: +86-43185262866. Fax: +86-43185262126 (Y.Z.).

*E-mail: wjiang@ciac.ac.cn. Phone: +86-43185262151. Fax: +86-43185262126 (W.J.).

Notes

The authors declare no competing financial interest.

■ ACKNOWLEDGMENTS

This work was financially supported by the National Natural Science Foundation of China for Youth Science Funds (21104083), General Program (51373172, 51275055), Major Program (50930001), Research Fellowship for International Young Scientists (21250110518), and the Scientific Development Program of Jilin Province (201201007).

■ REFERENCES

(1) Moniruzzaman, M.; Winey, K. I. *Macromolecules* **2006**, *39*, 5194−5205.
(2) Alig, I.; Pötschke, P.; Lellinger, D.; Skipa, T.; Pegel, S.; Kasaliwal, G. R.; Villmow, T. *Polymer* **2012**, *53*, 4−28.
(3) Tawfick, S.; De Volder, M.; Copic, D.; Park, S. J.; Oliver, C. R.; Polsen, E. S.; Roberts, M. J.; Hart, A. J. *Adv. Mater.* **2012**, *24*, 1628−1674.
(4) de Heer, W. A.; Bacsa, W. S.; Châtelain, A.; Gerfin, T.; Humphrey-Baker, R.; Forro, L.; Ugarte, D. *Science* **1995**, *268*, 845−847.
(5) Hinds, B. J.; Chopra, N.; Rantell, T.; Andrews, R.; Gavalas, V.; Bachas, L. G. *Science* **2004**, *303*, 62−65.
(6) Lu, J. R.; Weng, W. G.; Chen, X. F.; Wu, D. J.; Wu, C. L.; Chen, G. H. *Adv. Funct. Mater.* **2005**, *15*, 1358−1363.
(7) Lanticse, L. J.; Tanabe, Y.; Matsui, K.; Kaburagi, Y.; Suda, K.; Hoteida, M.; Endo, M.; Yasuda, E. *Carbon* **2006**, *44*, 3078−3086.
(8) Cebeci, H.; de Villoria, R. G.; Hart, A. J.; Wardle, B. L. *Compos. Sci. Technol.* **2009**, *69*, 2649−2656.
(9) Liu, S.; Liu, Y.; Cebeci, H.; de Villoria, R. G.; Lin, J. H.; Wardle, B. L.; Zhang, Q. M. *Adv. Funct. Mater.* **2010**, *20*, 3266−3271.
(10) Ok, J. G.; Tawfick, S. H.; Juggernauth, K. A.; Sun, K.; Zhang, Y. Y.; Hart, A. J. *Adv. Funct. Mater.* **2010**, *20*, 2470−2480.
(11) Yun, S. H.; Yoo, S. M.; Sohn, B. H.; Jung, J. C.; Zin, W. C.; Kwak, S. Y.; Lee, T. S. *Langmuir* **2005**, *21*, 3625−3628.
(12) Braun, E.; Eichen, Y.; Sivan, U.; Ben-Yoseph, G. *Nature* **1998**, *391*, 775−778.
(13) Tang, Z. Y.; Kotov, N. A. *Adv. Mater.* **2005**, *17*, 951−962.
(14) Li, B.; Jung, H. Y.; Wang, H. L.; Kim, Y. L.; Kim, T.; Hahm, M. G.; Busnaina, A.; Upmanyu, M.; Jung, Y. J. *Adv. Funct. Mater.* **2011**, *21*, 1810−1815.
(15) Jin, S.; Tiefel, T. H.; Wolfe, R.; Sherwood, R. C.; Mottine, J. J. *Science* **1992**, *255*, 446−448.
(16) Prasse, T.; Cavaillé, J. Y.; Bauhofer, W. *Compos. Sci. Technol.* **2003**, *63*, 1835−1841.
(17) Martin, C. A.; Sandler, J. K. W.; Windle, A. H.; Schwarz, M.-K.; Bauhofer, W.; Schulte, K.; Shaffer, M. S. P. *Polymer* **2005**, *46*, 877−886.
(18) Valentini, L.; Bon, S. B.; Kenny, J. M. *Macromol. Mater. Eng.* **2008**, *293*, 867−871.
(19) Cardinali, M.; Valentini, L.; Kenny, J. M. *J. Phys. Chem. C* **2011**, *115*, 16652−16656.
(20) Kim, I. T.; Tannenbaum, A.; Tannenbaum, R. *Carbon* **2011**, *49*, 54−61.
(21) Kim, I. T.; Lee, J. H.; Shofner, M. L.; Jacob, K.; Tannenbaum, R. *Polymer* **2012**, *53*, 2402−2411.
(22) Oliva-Avilés, A. I.; Avilés, F.; Sosa, V.; Oliva, A. I.; Gamboa, F. *Nanotechnology* **2012**, *23*, 465710.
(23) Shen, J.; Zhu, Y.; Zhou, K.; Yang, X.; Li, C. *J. Mater. Chem.* **2012**, *22*, 545−550.
(24) Mao, C.; Huang, J. R.; Zhu, Y. T.; Jiang, W.; Tang, Q. X.; Ma, X. J. *J. Phys. Chem. Lett.* **2013**, *4*, 43−47.
(25) Zhu, Y. T.; Yang, X. D.; Yin, J. H.; Jiang, W. *Phys. Rev. E* **2010**, *82*, 031807.
(26) Lin-Gibson, S.; Pathak, J. A.; Grulke, E. A.; Wang, H.; Hobbie, E. K. *Phys. Rev. Lett.* **2004**, *92*, 048302.
(27) Montesi, A.; Peña, A. A.; Pasquali, M. *Phys. Rev. Lett.* **2004**, *92*, 058303.
(28) Osuji, C. O.; Weitz, D. A. *Soft Matter* **2008**, *4*, 1388−1392.
(29) Negi, A. S.; Osuji, C. O. *Rheol. Acta* **2009**, *48*, 871−881.